Effects of Osmotic Pressure and Adsorption on Ultrafiltration of Ovalbumin

The influence of osmotic pressure and solute adsorption on permeate flux during ultrafiltration of a solute that forms a gel-like layer on membrane surfaces was investigated. Ovalbumin solutions were ultrafiltrated using three different kinds of membranes, polyolefine, polysulfone, and polyacrylonitrile. Flux data were analyzed by three conventional models: gel polarization, osmotic pressure, and resistance in series.

The experimental data were in conflict with all conventional models. Data analysis suggested that the main factors which influence permeate flux decline were osmotic pressure increase at the membrane surface and resistance caused by solute adsorption.

A new model, which takes into account both osmotic pressure and resistance due to solute adsorption, is proposed. Permeate flux declines observed in the experiments fit this model quite precisely. The gel layer that forms on the membrane surface has little influence on permeate flux and can be neglected.

Hiroshi Nabetani
Mitsutoshi Nakajima
Atsuo Watanabe
National Food Research Institute
Ministry of Agriculture, Forestry, and Fisheries
Kan-nondai, Tsukuba, Ibaraki, 305, Japan

Shin-ichi Nakao
Shoji Kimura
Department of Chemical Engineering
Faculty of Engineering
University of Tokyo
Hongo, Bunkyo-ku, Tokyo, 113, Japan

Introduction

Permeate flux observed during ultrafiltration of macromolecular solutions is usually analyzed by use of one of three models: the gel polarization model (Baker and Strathman, 1970; Blatt et al., 1970; Porter, 1972; Nakao et al., 1979; Probstein et al., 1978; Shen and Probstein, 1977; Trettin and Doshi, 1980), the osmotic pressure model (Goldsmith, 1971; Kozinski and Lightfoot, 1971, 1972; Clifton et al., 1984; Leung and Probstein, 1979; Mitra and Lundblad, 1978; Trettin and Doshi, 1981; Vilker et al., 1981b; Wijmans et al., 1985), or the resistance-in-series model (Chiang and Cheryan, 1986).

In membrane separation processes, solutes that are rejected by the membrane accumulate on the membrane surface. The concentration of solutes on the membrane surface is always higher than in the bulk solution. This is the so-called concentration polarization phenomenon.

According to the gel polarization model, solutes accumulate on the membrane surface and form a gel layer there. Permeate flux is reduced by the hydraulic resistance of the gel layer. Macromolecular solutes, for example proteins, tend to form gels at high concentration. The gel layer can be observed on the membrane surface after ultrafiltration of such solutes (Nakao et al., 1979; Koutake et al., 1987).

In the osmotic pressure model, permeate flux reduction results from the decrease in effective transmembrane pressure that occurs as the osmotic pressure of the retentate increases. This model was first applied to the analysis of reverse osmosis data (Kimura and Sourirajan, 1967). Recently, both theoretical (de Gennes, 1979) and experimental (Wales, 1981; Vilker et al., 1981a) studies show that osmotic pressure of macromolecular solutions increases with concentration in a nonlinear manner. During ultrafiltration of macromolecular solutions, the concentration polarization phenomenon increases solute concentration at the membrane surface to such a degree that osmotic pressure at the membrane surface is no longer negligible. Flux data are often analyzed by the osmotic pressure model.

The influence of macromolecular solute adsorption on the pure water permeability and rejection ability of ultrafiltration membranes has been studied. This influence can be significant, depending on the type of membrane (Matthiasson, 1983; Nabetani et al., 1988). In the resistance-in-series model, permeate flux decreases as a function of the resistances caused by both fouling phenomena (solute adsorption, etc.) and concentration polarization/gel layer formation. The latter resistance is proportional to applied pressure and the former is independent of pressure.

In this study, the influence of resistances caused by solute adsorption and by osmotic pressure at the membrane surface on permeate flux decline during ultrafiltration of macromolecular solute were evaluated independently. A new model, which takes into account osmotic pressure and adsorption effects, was developed. According to this model, flux predictions fit observed flux data quite precisely.

For this study, a simple method to determine resistance caused by solute adsorption was developed, as was a new apparatus for measuring osmotic pressures of macromolecular solutions.

The solute used was ovalbumin, which has been used in many studies as a solute that forms a gel layer on the surface of ultrafiltration membranes (Nakao et al., 1979, 1982; Nakao and Kimura, 1981a; Ohtani et al., 1985). Three kinds of ultrafiltration membranes—polyolefine, polysulfone, and polyacrylonitrile—were used.

Theory

Gel polarization model

The concentration polarization phenomenon may be quantified by Eq. 1 (Kimura and Sourirajan, 1967; Blatt et al., 1970).

$$\frac{C_m - C_p}{C_b - C_p} = \exp\frac{J_v}{k} \tag{1}$$

where J_v and k are permeate flux and mass transfer coefficient, respectively, and C_m, C_p, and C_b are solute concentrations on the membrane surface, in permeate, and in bulk retentate, respectively.

The gel polarization model may be described in a manner similar to that of the concentration polarization model. When the membrane surface concentration is very high and a gel layer is formed, gel layer concentration C_g is employed instead of C_m. Then J_v can be expressed as

$$J_v = k \cdot \ln\frac{C_g - C_p}{C_b - C_p} \tag{2}$$

Since the rejection ability of an ultrafiltration membrane for macromolecules is generally very high, especially when a gel layer is formed on the membrane surface (Nakao and Kimura, 1981a; Nakao et al., 1982), the term C_p can be neglected. Then

$$J_v = k \cdot \ln\frac{C_g}{C_b} \tag{3}$$

In this model, gel layer concentration is assumed to be constant and dependent only on the kind of solutes, not on experimental conditions such as feed velocity and pressure. Therefore, under the conditions in which a gel layer is formed, Eq. 3 predicts a linear plot of J_v vs. $\ln C_b$ with a slope equal to $-k$. Extrapolation to $J_v = 0$ yields the $\ln C_g$ value. It also implies that J_v is a functioin of neither the membrane's intrinsic resistance nor of applied pressure, as long as a gel layer is formed. Since the J_v value obtained from Eq. 3 is independent of applied pressure it is often called the limiting flux, $J_{v,\lim}$.

Osmotic pressure model

In the osmotic pressure model, effective driving pressure is reduced as the osmotic pressure of the retentate increases, and flux therefore declines, according to Eq. 4.

$$J_v = L_p(\Delta P - \sigma \cdot \Delta\Pi) \tag{4}$$

where ΔP, σ, and $\Delta\Pi$ are applied pressure, reflection coefficient, and osmotic pressure difference across the membrane, respectively. L_p is the pure water permeability of the membrane. When rejection is sufficiently high, σ can be assumed to be unity and osmotic pressure difference across the membrane can be determined by the concentration at the membrane surface as

$$\Delta\Pi = \Pi(C_m) - \Pi(C_p) \simeq \Pi(C_m) \tag{5}$$

and Eq. 1 can be written as

$$C_m = C_b \exp\frac{J_v}{k} \tag{6}$$

The osmotic pressure of a macromolecular solution can be represented as

$$\Pi(C) = A_1 \cdot C + A_2 \cdot C^2 + A_3 \cdot C^3 \tag{7}$$

where A_1, A_2, and A_3 are constants. Using Eqs. 5 and 7, Eq. 4 can be rewritten as

$$J_v = L_p[\Delta P - (A_1 \cdot C_m + A_2 \cdot C_m^2 + A_3 \cdot C_m^3)] \tag{8}$$

When k, and L_p, A_1, A_2, and A_3 are known, the value of J_v can be obtained by use of Eqs. 6 and 8.

Mass transfer coefficient k is generally calculated using a mass transfer correlation, as a function of flow velocity, height of flow channel, diffusion coefficient of solute, and kinematic viscosity of solution. The mass transfer coefficient can also be measured experimentally using the velocity variation method (Jonsson and Boesen, 1977; Nakao and Kimura, 1981b).

When pure water is ultrafiltrated, there is no effect of osmotic pressure in Eq. 4, and pure water permeability L_p is obtained by substituting pure water permeate flux J_w in Eq. 9:

$$J_w = L_p \cdot \Delta P \tag{9}$$

Resistance-in-series model

In the resistance-in-series model, permeate flux J_v may be expressed as

$$J_v = \frac{\Delta P}{R_m + R_f + R_p} \tag{10}$$

where R_p and R_f are respectively the resistances due to the concentration polarization/gel layer and those due to other fouling phenomena such as solute adsorption. The intrinsic resistance of a membrane, R_m, can be calculated from pure

water permeability L_p:

$$R_m = \frac{1}{L_p} = \frac{\Delta P}{J_w} \tag{11}$$

The permeate resistance R_p is assumed to be proportional to the amount and the specific hydraulic resistance of the deposited layer on the membrane. When applied pressure is increased, the thickness of the gel layer grows because the flux temporarily increases without a corresponding increase in the mass transfer coefficient. R_p is, therefore, a function of pressure:

$$R_p = \phi \cdot \Delta P \tag{12}$$

where ϕ is a constant for a particular membrane-solute combination. Thus Eq. 10 can be rewritten as

$$J_v = \frac{\Delta P}{R_m + R_f + \phi \cdot \Delta P} \tag{13}$$

Since R_f is considered independent of pressure, when ΔP is low, J_v is controlled by $(R_m + R_f)$, and when ΔP is high the effect of $(R_m + R_f)$ becomes less and the permeate flux would approach the value of $1/\phi$. ϕ would then become a function of bulk concentration and feed velocity, both affecting the mass transfer characteristics of the system. Permeate flux at infinite pressure $J_{v,\infty}$ $(=1/\phi)$, therefore, should not be affected by the kind of membrane.

Experimental Method

Apparatus and materials

Two kinds of ultrafiltration apparatus were employed. One was a batch-type cell (Ulvac Service Corp., type MC-2A). The effective membrane area was 12 cm^2 and the cell volume was 100 mL, Figure 1.

The other was a crossflow filtration apparatus equipped with a plate and frame type module (Mitsui Petrochemical Industries, type UFP-2) and a high-pressure pump with variable speed motor. The flowsheet is shown in Figure 2. The effective membrane length, width, and height of the flow channel of the module were 14.7, 7.1, and 0.16 cm, respectively.

To measure the osmotic pressure of macromolecular solutions, a modified version of the membrane osmometer cell (Vilker et al., 1981a) was employed. The configuration of the osmometer cell is shown in Figure 3; it consists of two chambers, one for solvent and the other for solution. The chambers are separated by a membrane that is impermeable to the solute but permits free passage of water.

Diffusion coefficient of ovalbumin was measured using an analytical ultracentrifuge (Hitachi, Ltd., UCA-1A).

Three different ultrafiltration membranes, made of polysulfone (PS), polyolefine (PO), and polyacrylonitrile (PAN), were employed, Table 1.

Ovalbumin (MW 45,000) was supplied by Syuzui Hikotarou Syouten.

Three kinds of dextrans, T10 (MW 10,000), T40 (MW 40,000), and T70 (MW 70,000) were supplied by Pharmacia Fine Chemicals. The diffusion coefficient D of each dextran at

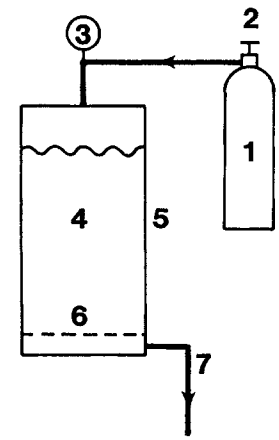

1. nitrogen gas
2. pressure control valve
3. pressure gauge
4. feed water
5. ultrafiltration cell
6. ultrafiltration membrane
7. permeate water

Figure 1. Flow diagram of experimental apparatus, batch-type ultrafiltration cell.

25°C is 10.5×10^{-11}, 5.4×10^{-11}, and 4.1×10^{-11} $m^2 \cdot s^{-1}$, respectively (Ohya et al., 1989).

Experimental conditions and procedure

Using a batch-type cell, changes in pure water permeability caused by adsorption of ovalbumin were measured. A new

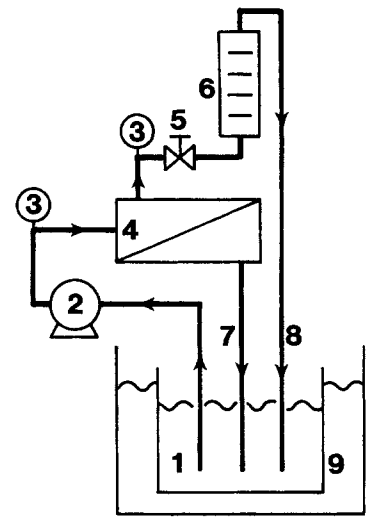

1. feed tank
2. pump
3. pressure gauge
4. ultrafiltration module
5. pressure control valve
6. flow meter
7. permeate
8. concentrate
9. thermostat

Figure 2. Flow diagram of crossflow apparatus.

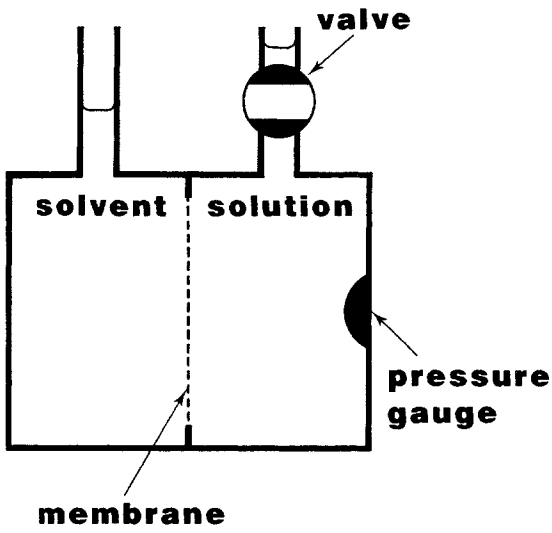

Figure 3. Configuration of osmometer cell.

membrane was placed in the cell and intrinsic pure water flux J_w was measured. The membrane was removed from the cell and soaked in ovalbumin solution. The membrane was placed in the cell again and pure water flux was measured. This procedure was repeated until a constant flux was obtained. The temperatures of the ovalbumin solution and the pure water were controlled at 25°C and pressure was maintained at 300 kPa by using nitrogen gas. Three concentrations of ovalbumin solution were employed, 0.1, 0.5, and 1.0 wt. %.

The osmotic pressure of ovalbumin solutions (concentrations 0–30 wt. %) was measured using the osmometer cell. The solution chamber was filled with ovalbumin solution and the valve was closed to prevent dilution of the solution caused by inflow of the solvent through the membrane. The solvent chamber was then filled with pure water. The increase in pressure in the solution chamber was monitored by a pressure gauge until the pressure reached a constant value. This pressure was regarded as the osmotic pressure of the solution. The temperature of the osmometer was controlled at 25°C.

The diffusion coefficient of ovalbumin was measured using an analytical ultracentrifuge at 25°C (Kawahara, 1968).

The mass transfer coefficient in the crossflow module was measured using the velocity variation method with three different kinds of dextrans, T10, T40, and T70. A dextran solution was ultrafiltrated at five different flow velocities from 0.15 to 0.75 $m \cdot s^{-1}$, corresponding to Reynolds numbers of 520 to 2,600. Permeate and feed were collected at each velocity and their dextran concentrations determined by the phenol–sulfuric acid method (Fukui, 1969). The observed rejection, R_{obs}, was calculated by the following equation:

$$R_{\text{obs}} = 1 - \frac{C_p}{C_b} \tag{14}$$

Table 1. Membranes Used in Study

Mfr.	Type	Material
NITTO	NTU-2120	Polyolefine (PO)
NITTO	NTU-3150	Polysulfone (PS)
DAICEL	DUY-HH	Polyacrylonitrile (PAN)

Two kinds of ultrafiltration membrane, made of polyolefine and polyacrylonitrile, were employed in this experiment. The pressure was controlled at 100 kPa and the concentration and temperature of feed solutions were constant at 0.01 wt. % and 25°C, respectively.

For ultrafiltration of ovalbumin solutions, the experimental conditions were as follows:

Feed concentration, 0.1, 0.5, 1.0 wt. %
Pressure, 100, 200, 300, 400 kPa
Flow velocity, 0.15, 0.27, 0.45, 0.81 $m \cdot s^{-1}$
Feed temperature, 25°C

Three different kinds of ultrafiltration membrane, made of polysulfone (PS), polyolefine (PO), and polyacrylonitrile (PAN), were employed. After circulating distilled water and reaching steady state, feed water was replaced with ovalbumin solution. Permeate fluxes and observed rejections were measured under each ultrafiltration condition at steady state. The concentrations of feed and permeate were analyzed spectrophotometrically at 213 nm and the observed rejection, R_{obs}, was calculated using Eq. 14.

Results and Discussion

Pure water permeability decline caused by solute adsorption

Pure water flux decreased as the time the membranes were soaked in ovalbumin solution increased. Steady state was reached after two or three days. Values of pure water flux before adsorption, J_w, and after reaching adsorption equilibrium, $J_{w,ad}$, are shown in Table 2, where C_b indicates the concentration of the solution in which the membranes were soaked. Soaking in more concentrated ovalbumin solution resulted in lower values of $J_{w,ad}$. This tendency depended on the membrane type. The value of $(J_w/J_{w,ad})$ obtained using PAN membrane was the highest among the three kinds of membranes tested.

Osmotic pressure of ovalbumin solution

Values of pressure in the solution chamber reached steady state within 5–6 h and measuring time was shortened compared with the conventional apparatus (Vilker et al., 1981a), which requires nearly one day to reach steady state.

The osmotic pressure of ovalbumin solutions measured using the osmometer cell is shown in Figure 4. From these data Eq. 15 was obtained:

$$\Pi(C) = 3.55 \times 10^3\, C + 8.34\, C^3 \tag{15}$$

This equation was used to construct the curve shown in Figure 4.

Table 2. Pure Water Flux

Membrane	J_w^*	$J_{w,ad}^{**}$ $C_b = 0.1$	$C_b = 0.5$	$C_b = 1.0$
PO	64.2	54.6	35.1	27.7
PS	163.2	41.1	39.0	32.4
PAN	69.6	11.6	5.73	5.01

*Before adsorption treatment $\times 10^{-6}\ m^3 \cdot m^{-2} \cdot s^{-1}$
**After reaching adsorption equilibrium $\times 10^{-6}\ m^3 \cdot m^{-2} \cdot s^{-1}$
C_b, bulk solute concentration, wt. %
$\Delta P = 300$ kPa

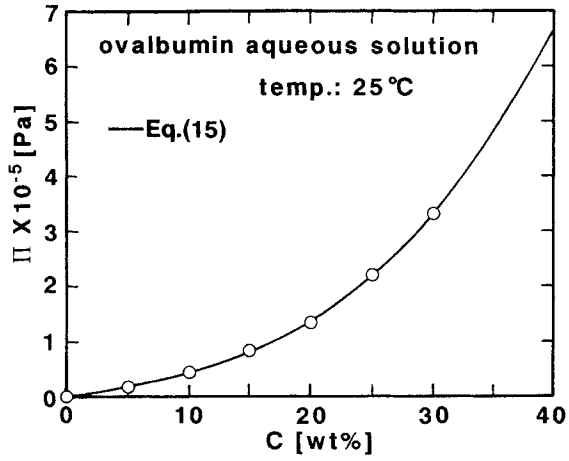

Figure 4. Osmotic pressure of ovalbumin aqueous solution.
Line calculated by Eq. 15

Obtained osmotic pressure of dextran T70 solutions is also shown in Figure 5. The values were in good agreement with the data offered by Wijmans et al. (1985). The accuracy of the measurement by the membrane osmometer cell was, therefore, confirmed.

Diffusion coefficient of ovalbumin

The measured diffusion coefficient D of ovalbumin in water at 25°C was nearly independent of solute concentration in the concentration range 0.1 to 1.5 wt. %. A value of 6.9×10^{-11} $m^2 \cdot s^{-1}$ was obtained.

Mass transfer coefficient in the module

The mass transfer coefficient in the concentration polarization layer is usually obtained using the mass transfer correlation, the so-called Leveque equation, when the flow in the module is laminar (Blatt et al., 1970):

$$Sh = \left(1.62 \frac{Re\, Sc\, d_h}{L^{1/3}}\right)^{1/3} \tag{16}$$

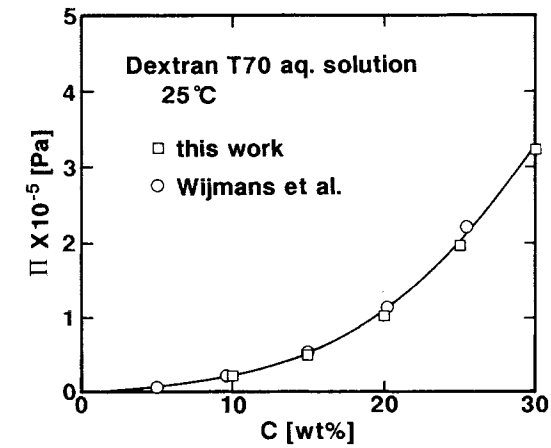

Figure 5. Osmotic pressure of dextran T70 aqueous solution.

For the module used in this study, the configuration of the flow channel is flat rectangular, where d_h is defined as

$$d_h = \frac{4a\,h}{[2(a+h)]} \tag{17}$$

and where a and h are channel width and height, respectively.

In Figure 6, mass transfer coefficients measured by the velocity variation method (plots) were compared with the Leveque equation (solid line). The experimental data agreed well with Eq. 16, and proved that, for the module used in this study, mass transfer coefficient for another solute could be calculated using this equation.

Ultrafiltration of ovalbumin solution

Values of permeate flux decreased with time and reached steady state within 1–2 h. The values of observed rejection, R_{obs}, were unity in all experiments. After ultrafiltration of ovalbumin solution, a gel-like layer was observed on all membrane surfaces.

Analysis by the gel polarization model

Experimental flux data were first analyzed using the gel polarization model. Relationships between applied pressure and permeate flux are shown in Figure 7, where bulk concentration and feed flow velocity were 1.0 wt. % and 0.81 $m \cdot s^{-1}$, respectively. Permeate flux was almost independent of applied pressure at values greater than 300 kPa. Limiting flux, $J_{v,lim}$, was observed for all membrane types. However, the values of $J_{v,lim}$ differed depending on the type of membrane, with the value for the PAN membrane being less than those observed for the others. This result was inconsistent with the gel polarization model, according to which the value of $J_{v,lim}$ should not depend on membrane resistance.

Relationships between ln C_b and J_v values at 400 kPa (which could be assumed to be $J_{v,lim}$) are shown in Figure 8, where the flow rate was 0.81 $m \cdot s^{-1}$. A plot of ln C_b vs. J_v is linear, but the gel layer concentrations C_g, which were obtained by extrapolation to the point of intersection with the ln C_b axis, differed

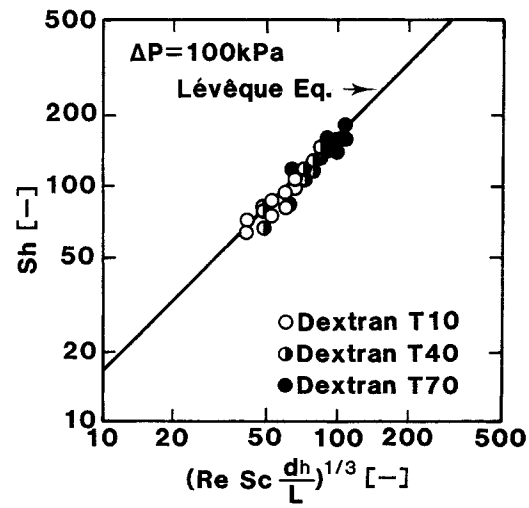

Figure 6. Experimental mass transfer coefficient and calculated values.

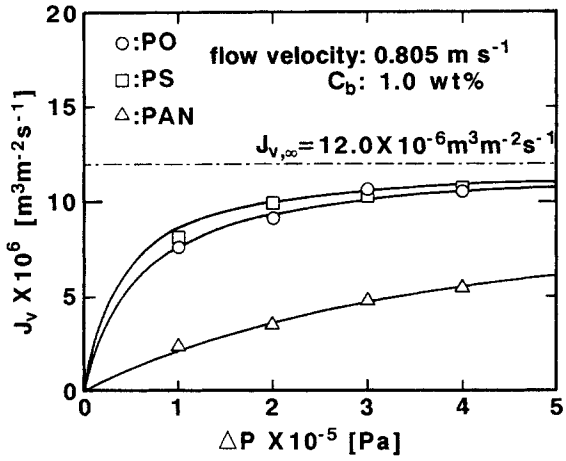

Figure 7. Relationships between applied pressure ΔP and permeate flux J_v for three kinds of membranes.
Lines obtained using resistance-in-series model

among the membranes. This phenomenon could not be explained by the gel polarization model.

Ovalbumin solutions, of concentration equivalent to C_g (obtained from Figure 8), could be prepared easily and while they were viscous, they were not like the gel-like deposit observed on the membrane surface. This result indicates that C_g values obtained by the gel polarization model for all the membranes do not imply the concentration of "gel" physically.

Analysis using the osmotic pressure model

Permeate flux data were then analyzed using the osmotic pressure model.

The mass transfer coefficient k at each flow velocity was calculated by substituting the D value of ovalbumin in Eq. 16. Pure water permeabilities L_p for each of the three membranes, which were obtained from pure water permeate fluxes J_w (Eq. 9), are shown in Table 3.

Using these L_p values and Eqs. 6, 8, and 15, volume permeate flux J_v was calculated. Calculated lines and the experimental

Table 3. Pure Water Permeability

Membrane	L_p^*	$L_p'^{**}$ $C_b = 0.1$	$C_b = 0.5$	$C_b = 1.0$
PO	21.4	18.2	11.7	9.23
PS	54.4	13.7	13.0	10.8
PAN	23.2	3.87	1.91	1.67

*Before solute adsorption $\times 10^{-11}$ m³ · m⁻² · s⁻¹ · Pa⁻¹
**After solute adsorption $\times 10^{-11}$ m³ · m⁻² · s⁻¹ · Pa⁻¹
C_b, bulk solute concentration, wt. %

data are shown in Figure 9. Flow velocity and bulk concentration were 0.81 m · s^{-1} and 1.0 wt. %, respectively.

Although the experimental data for PO and PS membranes agreed closely with the calculated values, the data for the PAN membrane were lower. Under all other conditions tested, similar results were obtained.

It was concluded, therefore, that the behavior of permeate flux during ultrafiltration of ovalbumin could not be explained by simply using the osmotic pressure model.

Analysis by the resistance-in-series model

Data were then analyzed using the resistance-in-series model (Chiang et al., 1986). The data were fitted to Eq. 13 and two parameters, non-pressure-related resistance of fouled membranes, $R_m + R_f$, and permeate flux at infinite pressure, $J_{v,\infty}$ $(=1/\phi)$, were determined. Values of $R_m + R_f$ are shown in Table 4, together with values of intrinsic membrane resistance R_m, Eq. 11. The solid lines in Figure 7 were drawn by Eq. 13 and these parameters, where the value of $J_{v,\infty}$ was 12.0 $\times$ 10^{-6} m³ · m^{-2} · s^{-1}.

The increase in permeate resistance that results from solute adsorption, $R_m + R_a$, may be expressed as:

$$R_m + R_a = \frac{\Delta P}{J_{w,ad}} \tag{18}$$

where $J_{w,ad}$ is pure water flux measured with the membrane presoaked in ovalbumin solution to the point of equilibrium

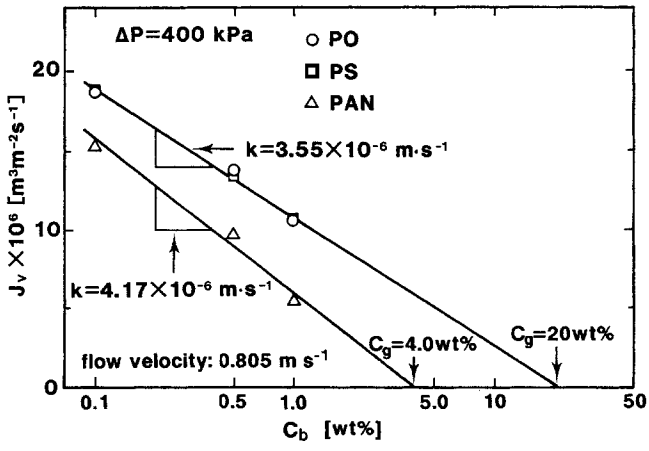

Figure 8. Relationships between log bulk concentration C_b and permeate flux J_v at applied pressure of 400 kPa.

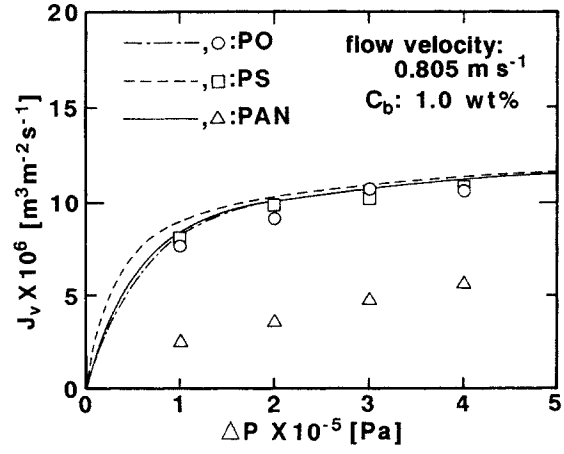

Figure 9. Experimental and calculated fluxes for three kinds of membranes.
Lines were calculated by Eqs. 6, 8, and 15 and L_p values in Table 3

Table 4. Membrane Permeate Resistance

Membrane	R_m^*	$R_m + R_f^{**}$	$R_m + R_a$†
		$C_b = 0.1$ wt. %	
PO	4.67	3.08	5.49
PS	1.84	3.55	7.30
PAN	4.31	7.16	25.8
		$C_b = 0.5$ wt. %	
PO	4.67	2.12	8.55
PS	1.84	2.49	7.69
PAN	4.31	11.6	52.4
		$C_b = 1.0$ wt. %	
PO	4.67	4.62	10.8
PS	1.84	3.27	9.26
PAN	4.31	38.1	59.9

All values $\times 10^9$ Pa · s · m^{-1}

*Intrinsic membrane permeate resistance

**Intrinsic resistance plus resistance due to fouling other than concentration polarization/gel layer; values obtained by fitting experimental data to Eq. 13

†Intrinsic resistance plus resistance due to solute adsorption; values obtained by Eq. 18

C_b, bulk solute concentration

adsorption. R_a is, therefore, permeate resistance caused only by solute adsorption. Values of $R_m + R_a$ are also shown in Table 4. Both $R_m + R_f$ and $R_m + R_a$ for the PAN membrane were the largest. In all cases, $R_m + R_a$ was larger than $R_m + R_f$. For the PO membrane, $R_m + R_f$ is less than R_m alone, implying negative values of R_f. With PS subtraction of R_m from $R_m + R_f$ values yield positive values for R_f, but they do not correlate with C_b in a logical manner. This indicates that the term $R_m + R_f$ does not represent the entire effect of solute adsorption. Thus the term R_p $(=\phi \cdot \Delta P)$ in Eq. 10 for the resistance-in-series model may include the effect of solute adsorption.

Analysis by the osmotic pressure and adsorption resistance model

Measurement of pure water flux decline caused by solute adsorption proved that this phenomenon has a significant influence on the pure water permeability of ultrafiltration membranes, especially the PAN type. The J_v values for PO and PS membranes, on which ovalbumin did not adsorb to the extent that it adsorbed on the PAN membrane, calculated by the osmotic pressure model agreed well with experimental data, as shown in Figure 9.

One reason the model could not predict permeate flux of the PAN membrane might be the absence of solute adsorption as a factor in the osmotic pressure model. The data were therefore analyzed by a new model, the osmotic pressure and adsorption resistance model.

The reduction in pure water permeability, L_p', caused by solute adsorption was calculated by Eq. 19:

$$L_p' = \frac{J_{w,ad}}{\Delta P} = \frac{1}{R_m + R_a} \tag{19}$$

Values of L_p' are shown in Table 3, where C_b indicates the concentrations of ovalbumin solution in which membranes were soaked. L_p' decreased with increase in C_b. The PAN membrane had the lowest L_p' of the three membranes tested.

Considering the influence of solute adsorption, Eq. 8 can be rewritten as

$$J_v = L_p' [\Delta P - (A_1 \cdot C_m + A_2 \cdot C_m^2 + A_3 \cdot C_m^3)] \tag{20}$$

Using Eqs. 6, 15, and 20, J_v was calculated and compared with experimental values, Figure 10, where filtration conditions were the same as those used for the data shown in Figure 7. Experimental values for all membranes agreed well with calculated values, and differences of permeate flux among the membranes could be predicted.

The relationship between calculated permeate flux, $J_{v,cal}$, and experimental permeate flux, $J_{v,exp}$, under all filtration conditions applied in this study is shown in Figure 11. Experimental values for all membranes agreed well with calculated values.

From these results, it was found that the behavior of permeate flux during ultrafiltration of ovalbumin solution can be explained by the osmotic pressure and adsorption resistance model newly developed in this study. Using this model, permeate flux can be predicted when mass transfer coefficient in the module, osmotic pressure of solution, and the reduction of pure water permeability caused by solute adsorption are all known. Furthermore, the importance of choosing membranes that do not exhibit solute adsorption was demonstrated quantitatively in this study, although this had already been suggested experimentally (Matthiasson, 1983; Fane et al., 1983, Nabetani et al., 1988).

The influence of the gel-like layer on permeate flux was found to be negligible, even though it was always observed on the membrane surface.

The osmotic pressure and adsorption resistance model proposed here provides good predictions of the pressure dependence of permeate flux, which cannot be explained by use of the gel polarization model.

Although data for the three kinds of membranes are predicted equally well by the resistance-in-series model and the osmotic pressure and adsorption resistance model, the superiority of the osmotic pressure and adsorption resistance model is that the parameters needed in the model can be estimated independently.

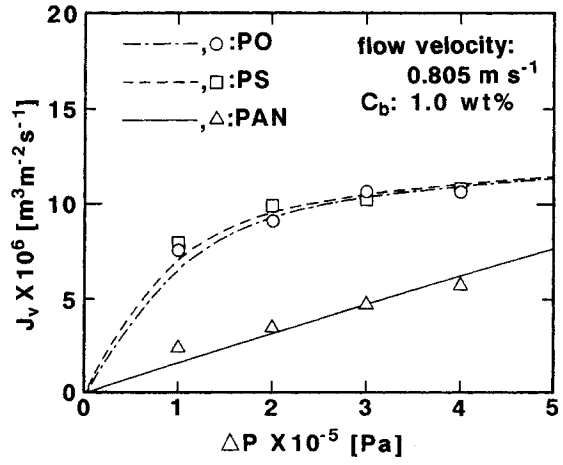

Figure 10. Experimental and calculated fluxes for three kinds of membranes.

Lines calculated by Eqs. 6, 15, and 20 and L_p' values in Table 3

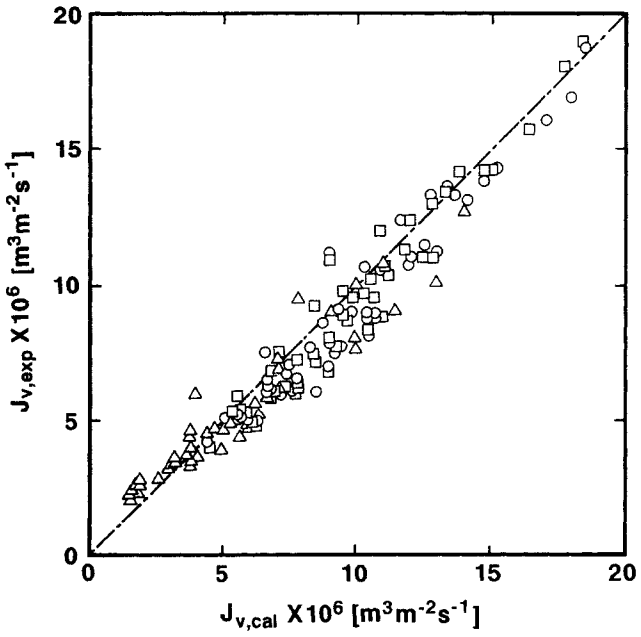

Figure 11. Relationship between calculated permeate flux $J_{v,cal}$ and experimental permeate flux $J_{v,exp}$ under all filtration conditions used in study.

$J_{v,cal}$ calculated by Eqs. 6, 15, and 20 and L_p' in Table 3
Symbols as in Figure 9

Conclusions

Ovalbumin solution was ultrafiltrated with polyolefine, polysulfone, and polyacrylonitrile membranes, under conditions of different bulk concentration, flow rate, and pressure.

A gel-like layer was always observed on the membrane surfaces, but the behavior of volume permeate flux could not be explained by the conventional models (gel polarization, resistance-in-series, and osmotic pressure).

An osmotic pressure and adsorption resistance model, which considers the influence of solute adsorption on pure water permeability, is therefore proposed. Permeate fluxes calculated by this model agreed well with experimental data. The influence of the gel-like layer on volume permeate flux was negligible. Therefore, permeate flux during ultrafiltration of ovalbumin solution can be predicted by this model, when mass transfer coefficient in the module, osmotic pressure of the solution, and the reduction in pure water permeability that results from solute adsorption are defined.

Notation

a = width of flow channel of a module, m
A_1, A_2, A_3 = constants
C = solute concentration, wt. %
D = diffusion coefficient, m^2 · s^{-1}
d_h = equivalent hydraulic diameter, m
h = height of flow channel of a module, m
J_v = volume permeate flux, m^3 · m^{-2} · s^{-1}
$J_{v,lim}$ = limiting flux, m^3 · m^{-2} · s^{-1}
$J_{v,\infty}$ = permeate flux at infinite pressure, m^3 · m^{-2} · s^{-1}
J_w = pure water permeate flux, m^3 · m^{-2} · s^{-1}
$J_{w,ad}$ = pure water permeate flux after solute adsorption, m^3 · m^{-2} · s^{-1}
k = mas transfer coefficient, m · s^{-1}
L = length of flow channel of a module, m
L_p = pure water permeability, m^3 · m^{-2} · s^{-1} · Pa^{-1}
L_p' = pure water permeability after solute adsorption, m^3 · m^{-2} · s^{-1} · Pa^{-1}
P = pressure, Pa
R_a = permeate resistance due to solute adsorption, Pa · s · m^{-1}
R_f = permeate resistance due to fouling other than concentration polarization/gel layer, Pa · s · m^{-1}
R_m = permeate resistance of a membrane $= 1/L_p$, Pa · s · m^{-1}
R_p = permeate resistance due to concentration polarization/gel layer, Pa · s · m^{-1}
Re = Reynolds number $= u\,d_h/\nu$
R_{obs} = observed rejection
Sc = Schmidt number $= \nu/D$
Sh = Sherwood number $= k\,d_h/D$
u = flow velocity, m · s^{-1}

Greek letters

ν = kinematic viscosity, m^2 · s^{-1}
Π = osmotic pressure, Pa
σ = reflection coefficient
ϕ = constant

Subscripts

b = bulk
g = gel layer
m = membrane
p = permeate

Literature Cited

Baker, R. W., and H. Strathman, "Ultrafiltration of Macromolecular Solutions with High-flux Membranes," *J. Appl. Polym. Sci.*, **14,** 1197 (1970).

Blatt, W. F., A. Dravid, A. S. Michaels, and L. Nelson, "Solute Polarization and Cake Formation in Membrane Ultrafiltration: Causes, Consequence, and Control Techniques," *Membrane Science and Technology*, J. E. Flinn, ed., Plenum, New York, 47 (1970).

Chiang, B. H., and M. Cheryan, "Ultrafiltration of Skim Milk in Hollow Fibers," *J. Food Sci.*, **51,** 340 (1986).

Clifton, M. J., N. Abidine, P. Aptel, and V. Sanchez, "Growth of the Polarization Layer in Ultrafiltration with Hollow-Fiber Membranes," *J. Membrane Sci.*, **21,** 233 (1984).

de Gennes, P. G., *Scaling Concepts in Polymer Physics*, Conell Univ. Press, Ithaca (1979).

Fane, A. G., C. J. D. Fell, and A. G. Waters, "Ultrafiltration of Protein Solutions through Partially Permeable Membranes—The Effect of Adsorption and Solution Environment," *J. Membrane Sci.*, **16,** 211 (1983).

Fukui, S., *Quantitative Analysis Method of Reducing Sugars*, Tokyo Univ. Press, Tokyo, 45 (1969) (in Japanese).

Goldsmith, R. L., "Macromolecular Ultrafiltration with Microporous Membranes," *Ind. Eng. Chem. Fundam.*, **10,** 113 (1971).

Jonsson, G., and C. E. Boesen, "Concentration Polarization in a Reverse Osmosis Test Cell," *Desalination*, **21,** 1 (1977).

Kawahara, K., "Estimation of Diffusion Coefficient and Molecular Weight of Protein by Using Ultracentrifuge, *Protein, Nucleic Acid and Enzyme*, **13,** 798 (1968) (in Japanese).

Kimura, S., and S. Sourirajan, "Analysis of Data in Reverse Osmosis with Porous Cellulose Acetate Membranes Used," *AIChE J.*, **13,** 497 (1967).

Koutake, M., Y. Uchida, T. Sato, K. Shimoda, A. Watanabe, and S. Nakao, "Filtration Membrane Fouling in Ultrafiltration of Skim Milk. I: Causes and Cleaning, *Nippon Nougeikagaku Kaishi*, **61,** 677 (1987) (in Japanese).

Kozinski, A. A., and E. N. Lightfoot, "Ultrafiltration of Proteins in Stagnation Flow, *AIChE J.*, **17,** 81 (1971).

———"Protein Ultrafiltration: A General Experiment of Boundary Layer Filtration," *AIChE J.*, **18,** 1030 (1972).

Leung, W. F., and R. F. Probstein, "Low Polarization in Laminar Ultrafiltration of Macromolecular Solutions," *Ind. Eng. Chem. Fundam.*, **18,** 274 (1979).

Matthiasson, E., "The Role of Macromolecular Adsorption in Fouling of Ultrafiltration Membranes," *J. Membrane Sci.*, **16,** 23 (1983).

Mitra, G., and J. Lundblad, "Ultrafiltration of Immune Serum Globulin and Human Serum Albumin: Regression Analysis Studies," *Separ. Sci. Tech.*, **13**, 89 (1978).

Nabetani, H., M. Nakajima, A. Watanabe, S. Nakao, and S. Kimura, "Change of Permeate Flux and Solute Rejection by Ovalbumin Adsorption of Ultrafiltration Membranes," *Membrane*, **13**, 51 (1988) (in Japanese).

Nakao, S., and S. Kimura, "Effect of Gel Layer on Rejection and Fractionation of Different-Molecular-Weight Solutes by Ultrafiltration," *ACS Symp. Ser.*, **154**, 119 (1981a).

———"Analysis of Solute Rejection in Ultrafiltration," *J. Chem. Eng. Japan*, **14**, 32 (1981b).

Nakao, S., T. Nomura, and S. Kimura, "Characteristics of Macromolecular Gel Layer Formed on Ultrafiltration Tubular Membrane," *AIChE J.*, **25**, 615 (1979).

Nakao, S., S. Yumoto, and S. Kimura, "Analysis of Rejection Characteristics of Macromolecular Gel Layer for Low Molecular Weight Solutes in Ultrafiltration," *J. Chem. Eng. Japan*, **15**, 463. (1982).

Ohtani, T., A. Watanabe, C. Hoshino, and S. Kimura, "Application of Dynamic Membrane to Ultrafiltration,"*Kagaku Kougaku Ronbunshu*, **11**, 140 (1985) (in Japanese).

Ohya, H., C. Hashimoto, A. Haio, Y. Negishi, and K. Matsumoto, "Standardization Method for Molecular Weight Cutoff Evaluation of Ultrafiltration Membranes," *Membrane*, **14**, 88 (1989).

Porter, M. C., "Concentratin Polarization with Membrane Ultrafiltration," *Ind. Eng. Chem. Product Res. Devel.*, **11**, 234 (1972).

Probstein, R. F., J. S. Shen, and W. F. Leung, "Ultrafiltration of Macromolecular Solutions at High Polarization in Laminar Channel Flow," *Desalination*, **24**, 1 (1978).

Shen, J. S., and R. F. Probstein, "On the Prediction of Limiting Flux in Laminar Ultrafiltration of Macromolecular Solutions," *Ind. Eng. Chem. Fundam.*, **16**, 459 (1977).

Trettin, D. R., and M. R. Doshi, "Ultrafiltration in an Unstirred Batch Cell," *Ind. Eng. Chem. Fundam.*, **19**, 189 (1980).

———"Pressure-independent Ultrafiltration—Is It Gel Limited or Osmotic Pressure Limited?" *ACS Symp. Ser.*, **154**, 373 (1981).

Vilker, V. L., C. K. Colton, and K. A. Smith, "The Osmotic Pressure of Concentrated Protein Solutions: Effect of Concentration and pH in Saline Solutions of Bovine Serum Albumin," *J. Colloid Interf. Sci.*, **79**, 548 (1981a).

———"Concentration Polarization in Protein Ultrafiltration. II: Theoretical and Experimental Study of Albumin Ultrafiltrated in an Unstirred Cell," *AIChE J.*, **27**, 637 (1981b).

Wales, M., "Pressure Drop across Polarization Layers in Ultrafiltration," *ACS Symp. Ser.*, **154**, 159 (1981).

Wijmans, J. G., S. Nakao, and C. A. Smolders, "Hydrodynamic Resistance of Concentration Polarization Layer in Ultrafiltration," *J. Membrane Sci.*, **22**, 117 (1985).

Manuscript received Dec. 8, 1989, and revision received Apr. 3, 1990.